DNA Research **18**, 39–52, (2011) doi:10.1093/dnares/dsq033
Advance Access Publication: 24 December 2010

Pseudo-Response Regulator (PRR) Homologues of the Moss *Physcomitrella patens*: Insights into the Evolution of the PRR Family in Land Plants

Santosh B. Satbhai[1], Takafumi Yamashino[2,*], Ryo Okada[1], Yuji Nomoto[2], Takeshi Mizuno[2], Yuki Tezuka[1], Tomonori Itoh[1], Mitsuru Tomita[1], Susumu Otsuki[1], and Setsuyuki Aoki[1,*]

Graduate School of Information Science, Nagoya University, Furo-cho, Chikusa-ku, Nagoya 464-8601, Japan[1] and School of Agriculture, Nagoya University, Furo-cho, Chikusa-ku, Nagoya 464-8601, Japan[2]

*To whom correspondence should be addressed. Tel. +81-52-789-4090. Fax. +81-52-789-4091. E-mail: yamasino@agr.nagoya-u.ac.jp (T.Y.); Tel/Fax. +81-52-789-5376. E-mail: aoki@is.nagoya-u.ac.jp (S.A.)

Edited by Satoshi Tabata
(Received 21 September 2010; accepted 30 November 2010)

Abstract

The pseudo-response regulators (PRRs) are the circadian clock component proteins in the model dicot *Arabidopsis thaliana*. They contain a receiver-like domain (RLD) similar to the receiver domains of the RRs in the His–Asp phosphorelay system, but the RLDs lack the phosphoacceptor aspartic acid residue invariably conserved in the receiver domains. To study the evolution of *PRR* genes in plants, here we characterize their homologue genes, *PpPRR1*, *PpPRR2*, *PpPRR3* and *PpPRR4*, from the moss *Physcomitrella patens*. In the phylogenetic analysis, *PpPRRs* cluster together, sister to an angiosperm *PRR* gene subfamily, illustrating their close relationships with the angiosperm *PRRs*. However, distinct from the angiosperm sequences, the RLDs of PpPRR2/3/4 exhibit a potential phosphoacceptor aspartic acid–aspartic acid–lysine (DDK) motif. Consistently, the PpPRR2 RLD had phosphotransfer ability *in vitro*, suggesting that PpPRR2 functions as an RR. The PpPRR1 RLD, on the other hand, shows a partially diverged DDK motif, and it did not show phosphotransfer ability. All *PpPRRs* were expressed in a circadian and light-dependent manner, with differential regulation between *PpPRR2/4* and *PpPRR1/3*. Altogether, our results illustrate that PRRs originated from an RR(s) and that there are intraspecific divergences among PpPRRs. Finally, we offer scenarios for the evolution of the *PRR* family in land plants.

Key words: circadian clock; His–Asp phosphorelay system; response regulator; pseudo-response regulator; *Physcomitrella patens*

1. Introduction

Circadian rhythms are endogenous biological oscillations with a period of 1 day, and they are controlled by an autonomous oscillator, the circadian clock.[1] This clock regulates the timing of metabolism, physiology and behaviour of organisms, coordinating them with environmental factors that cycle with the rotation of the earth.[1,2] The mechanisms of the eukaryotic clocks are proposed to be founded on interlocked autoregulatory loops between genes that function as components of the clock machinery, whereas the identities of these genes are largely different between animals, plants and fungi.[3] In the model dicot *Arabidopsis thaliana*, a representative set of such component genes is the *pseudo-response regulator* (*PRR*) gene family, which comprises five member genes, *TOC1* (also called *PRR1*)/*PRR3*/*PRR5*/*PRR7*/*PRR9*, which play regulatory roles at multiple nodes in the interlocked loops of the *A. thaliana* circadian network.[4] All the *PRR* genes are, largely based on phenotypic analyses of mutants, supposed to be functionally important in the *A. thaliana* circadian system.[5] Although phenotypic changes in a single mutation of each *PRR* gene are not large, combinations of mutations of different *PRR*s often result in stronger

phenotypes, e.g. essentially arrhythmic in an extreme case.[4]

PRRs share a conserved domain, the receiver-like domain (RLD), along with another domain CONSTANS/CONSTANS-LIKE/TOC1 (CCT). The RLD is similar to the receiver domain of the RRs in the histidine to aspartic acid (His–Asp) phosphorelay, a versatile signal transduction system in organisms from bacteria to eukaryotes other than animals.[5,6] In the His–Asp phosphorelay, a phosphate group is transferred from a histidine kinase (HK), via an intermediate signal transducer histidine-containing phosphotransmitter (HPt), down to a counterpart RR, thereby transducing various environmental and endogenous signals intracellularly.[6] An aspartic acid residue in the receiver domain of RRs is conserved as the phosphoacceptor site,[6] whereas the RLDs of all the *A. thaliana* PRRs lack this aspartic acid residue, and they carry a glutamic acid instead.[5,6] Consistent with this, Makino *et al.*[7] showed that the RLD of TOC1 did not undergo phosphotransfer *in vitro*.

Here, we hypothesize that the ancestors of PRRs were authentic RRs and they have lost the phosphorelay function through the course of evolution. If so, it is of particular interest to know in what evolutionary scenario PRRs lost the phosphorelay function, in order to understand the evolution of plant clock machineries. Homologue sequences of the *A. thaliana PRR* genes have recently been characterized in several other angiosperms.[8–15] Importantly, Corellou *et al.*[16] recently showed that the green alga *Ostreococcus tauri* has a *PRR* homologue sequence (*OtTOC1*) that functions as a master clock gene. The OtTOC1 protein carries a potential phosphoacceptor aspartic acid in its RLD,[16] indicating that the substitution of the aspartic acid to the glutamic acid is likely to date back to the period between the emergence of the green alga and the divergence of angiosperms. It would be informative, therefore, to characterize their homologues from non-angiosperm land plants, which cover a wide spectrum of phylogenetic groups.[17,18]

Physcomitrella patens, a species of Bryopsida (moss), one of the basal land plants,[17,18] diverged from vascular plant lineages at least 450 million years ago.[18] This moss is an attractive model plant because various molecular biology techniques such as targeted gene disruption have been well established.[19] In a recent study, we isolated and characterized two *P. patens* cDNAs *PpCCA1a* and *PpCCA1b* encoding moss homologues of *A. thaliana* CCA1/LHY. CCA1/LHY is a pair of paralogous single myb proteins, which function as another type of important component proteins in the *A. thaliana* circadian network.[3,4] Disruption experiments on *PpCCA1a* and *PpCCA1b* genes indicate that these two genes are functional counterparts of *CCA1/LHY*.[20] We also identified four candidate genes that encode PRR homologues in the *P. patens* genome database.[20–22] We isolated the full-length cDNA for one of these four moss *PRR* genes and showed that this gene is expressed in a circadian manner.[20] Very recently, Holm *et al.*[23] reported a survey of clock-associated genes on the *P. patens* genome database, including the four moss *PRRs*. They constructed an unrooted tree of plant PRR homologues, in which the four moss PRRs clustered independently from angiosperm PRR subfamilies.[23]

In this study, we isolated and characterized cDNAs for the remaining three moss *PRR* genes, for which gene structures were so far predicted only from the genomic sequences. Using experimentally validated sequences of the moss *PRR* cDNAs, we constructed a rooted phylogenetic tree, thereby clearly defining the evolution of plant PRRs. We also conducted biochemical characterization and expression analyses of the moss *PRRs*; the results of these experiments suggest that at least one of the moss PRRs functions as an authentic RR and that there are intraspecific divergences among the moss PRRs. Finally, we will discuss scenarios of the evolution and divergence of *PRR* homologue genes in land plants.

2. Materials and methods

2.1. Plant materials, growth conditions and light treatment

Physcomitrella patens ssp. *patens*[24] was maintained in 12-h light and 12-h dark cycles (12:12LD) under white fluorescent light (light intensity ~40 μmol m^{-2} s^{-1}) at 25°C. Protonemal and gametophore tissues were grown on BCDAT/G medium and BCD medium, respectively, both supplemented with 1 mM $CaCl_2$.[25] Protonemal cells were collected every 5–7 days and were ground with a homogenizer before application to new BCDAT agar plates. For light sources of the light induction experiments, the light-emitting diodes (STICK LED, Tokyo Rikakikai) were used for blue light ($\lambda_{max} = 470$ nm) and the red-emitting fluorescent tubes (FL20S-Re-66, Toshiba Lighting & Technology) filtered through a red plastic sheet (Acrylite102, Mitsubishi Rayon) for red light ($\lambda_{max} = 660$ nm). White light was provided by fluorescence lumps (FL20SS-W/18, Toshiba Lighting & Technology).

2.2. Identification and isolation of cDNAs covering the entire coding regions of PpPRRs

The 5′- and 3′-terminal portions of the *PpPRR2* and *PpPRR4* cDNAs were RACE-amplified using GeneRacer (Invitrogen) with primers based on the JGI database sequences. The amplified cDNA fragments were cloned into the pGEM-T Easy vector (Promega) and sequenced with DYEenamic ET terminator [GE

Healthcare (Former Amersham Biosciences)]. The middle region of each gene was amplified by RT-PCR with primers based on the RACE-amplified sequences. The entire regions of both cDNAs were amplified with KOD plus polymerase Ver.2 (TOYOBO), subjected to A-tailing by *Taq* polymerase (TAKARA Bio), cloned into the pGEM-T Easy vector and sequenced using a primer walking method. The *PpPRR3* cDNA that spans its entire coding region was amplified with KOD plus polymerase Ver.2 using primers based on the JGI database sequences. Nucleotide sequences were assembled by DNASIS software (Hitachi software engineering). All primer sets used are described in Supplementary file 1.

2.3. Phylogenetic analyses

Amino acid sequences of PRR homologues were aligned using the ClustalW program[26] and the numbers of amino acid substitutions between each pair of PRR proteins were estimated by the Jones–Taylor–Thornton (JTT) model[27] with the complete-deletion option. From the estimated numbers of amino acid substitutions, a phylogenetic tree was reconstructed using the minimum evolution (ME) method.[28] The bootstrap values were calculated with 1000 replications.[29] These procedures were all performed using MEGA4.1 software (http://www.megasoftware.net/index.html[30]). We also reconstructed a phylogenetic tree by the maximum-likelihood method using PhyML (http://atgc.lirmm.fr/phyml/[31]) applying the JTT model for amino acid substitutions. We obtained a similar phylogeny pattern with both the methods.

2.4. Semi-quantitative and quantitative RT-PCR analyses

Semi-quantitative RT-PCR (sqRT-PCR) analysis was performed as described previously.[20] We conducted preliminary experiments to improve its quantitativeness as follows. First, thermal cycle numbers were optimized so that signals from PCR products did not reach a plateau. Next, we confirmed that when various known relative amounts of cDNA for each tested gene were used as PCR templates, the amount of the PCR product of each reaction showed a linear relationship with that of the input cDNA. The primers and optimal cycle numbers for PCR are described in Supplementary file 1. Quantitative real-time PCR (qRT-PCR) analysis was performed as described previously.[32] The primers are same as those used in the qRT-PCR analysis (Supplementary file 1).

2.5. Construction of plasmids

To express the PpPRR1 and PpPRR2 RLD peptides in *E. coli* cells, a cold shock expression system (pCold-II vector; TAKARA Bio) was used as follows. The coding region for the RLD of each PpPRR protein was PCR-amplified with primers described in Supplementary file 1. The resultant fragment was cloned into the pGEM-T Easy vector, digested with *Kpn*I and *Xba*I and inserted into *Kpn*I–*Xba*I-cleaved pCold-II vector (pCold-II-His-PRR1 and pCold-II-His-PRR2 for PpPRR1 RLD and PpPRR2 RLD, respectively). The nucleotide sequence was determined by DYEenamic ET terminator. The RLD peptides are fused with a 6×His-tag, by expression from pCold-II vector, allowing their purification with a TALON™ metal affinity resin column as described below.

2.6. Expression and purification of the PpPRR1 and PpPRR2 RLD peptides

The *E. coli* strain BL21 (DE3) harbouring pG-KJE8 (TAKARA Bio), which encodes chaperone proteins DnaK, DnaJ, GrpE, GroEL and GroES, was transformed with pCold-II-His-PRR1 or pCold-II-His-PRR2. To overproduce the RLD peptides of PpPRR1 and PpPRR2, each transformant was cultivated in 1 l of LB medium containing ampicillin (50 $\mu g\,ml^{-1}$), Chloramphenicol (25 $\mu g\,ml^{-1}$), tetracycline (20 $ng\,ml^{-1}$) and L-arabinose (10 $mg\,ml^{-1}$) at 37°C until the logarithmic phase of growth in a rotary shaker (at 110 r.p.m.). They were cold-shocked by standing at 15°C for 30 min after the addition of IPTG at the final concentration of 1 mM and cultured in a shaker (at 110 r.p.m.) at 15°C for 5 h. Cells were collected by centrifugation and suspended in 20 ml of a standard buffer [50 mM Tris–HCl (pH 8.0), 100 mM NaCl and 10% glycerol]. The cell suspension was mixed with DNase I (25 $\mu g\,ml^{-1}$), EDTA (1.25 mM) and lysozyme (250 $\mu g\,ml^{-1}$) at 4°C for 15 min, and then passed through a French Press at 100 MPa. The resultant cell lysate was centrifuged and separated from cell debris and then applied onto a TALON™ metal affinity resin (Clontech Laboratories) column. After washing the TALON™ column with 50 mM Tris–HCl (pH 8.0), 10% glycerol and 100 mM NaCl, each of 6×His-tagged PpPRR1 and PpPRR2 RLD peptides was eluted with the same buffer including 250 mM imidazole and finally dialysed against 50 mM Tris–HCl (pH 8.0) and 10% glycerol. Dialysed semi-purified protein was concentrated by loading on Amicon Ultra Filter (Ultracel-10K, Millipore) and centrifuged for 15 min at 4700 r.p.m. at 4°C. The sample was quantified by the Lowry method[33] and subjected to SDS–PAGE and detected with Coomassie Brilliant Blue. It was also analysed by western blotting with anti-6×His antibodies (Cat. No. A190-114A, Bethyl Laboratories).

2.7. Preparation of the E. coli *ArcB-enriched cytoplasmic membrane*

Escherichia coli DAC903/pIA001-ArcB and DAC903/pIN-III were used as an ArcB overproducer and a

negative control, respectively.[34] From each strain, membrane vesicles were isolated and pelleted as an insoluble fraction of the cell lysate according to the method of Azuma *et al*.[35] They were suspended in a small volume of a buffer comprising 50 mM Tris-acetate (pH 8.0), 1 mM DTT, 2% glycerol and 250 mM sucrose in order to isolate cytoplasmic membrane as follows. The suspended membrane vesicles were layered over a 21-ml five steps gradient of sucrose dissolved in the same buffer (3 ml of 50%, 9 ml of 45%, 3 ml of 40%, 3 ml of 35% and 3 ml of 30% from bottom to top) in a bottle assembly polycarbonate tube (part no. 355618, Beckman Coulter) and centrifuged at 47 000 r.p.m. for 2 h at 4°C with the type 50.2 Ti rotor (Beckman Coulter). The cytoplasmic membrane was collected by taking the fraction between the layers of 35 and 40% sucrose and diluted with a large volume of a buffer (T_AGS-buffer) comprising 50 mM Tris-acetate (pH 7.8), 1 mM DTT, 10% glycerol, 100 mM sucrose. The cytoplasmic membrane was collected by centrifugation at 127 000*g* for 2 h and then resuspended in a small volume of T_AGS-buffer. Finally, F_1-ATPase was stripped from the cytoplasmic membrane as follows. The isolated cytoplasmic membrane (2 mg of protein) was treated with 1 ml of T_AGS-buffer containing 4 M urea for 30 min on ice, and then recovered by centrifugation at 50 000 r.p.m. for 30 min. Then, the pellet was washed once with 1 ml of TGS buffer and finally with 1 ml of a buffer comprising 50 mM Tris–HCl (pH 8.0), 2 mM DTT and 10% glycerol. The urea-treated cytoplasmic membrane was suspended in 0.5 ml of the same buffer and stored at −80°C.

2.8. In vitro *autophosphorylation assay*

In vitro autophosphorylation reaction of the ArcB protein was carried out according to the method of Azuma *et al*.,[35] 4.0 μg of ArcB-enriched *Escherichia coli* cytoplasmic membrane was incubated with 0.05 mM γ-[^{32}P]-ATP (37 kBq) in TEG buffer (50 mM Tris–HCl, pH 8.0, 0.35 mM EDTA, 10% glycerol) containing 5 mM $MgCl_2$, 200 mM KCl and 2 mM DTT at 25°C for 1, 5 and 10 min. Four micrograms of *E. coli* cytoplasmic membrane, which was prepared from the strain which does not overproduce ArcB, was also used as a negative control experiment. The reaction was terminated by the addition of SDS–PAGE sample buffer [finally 20 mM Tris–HCl (pH 8.0), 1% β-mercaptoethanol, 1% SDS, 6% glycerol and 0.02% Bromophenol Blue]. The samples were subjected to SDS–PAGE. The gel was dried and analysed with an imaging scanner (BAS-2500; Fuji Film).

2.9. In vitro *His–Asp phosphotransfer assay*

In vitro His–Asp phosphotransfer reaction from ArcB to the RLD peptides of PpPRR1 and PpPRR2 was examined according to the method of Azuma *et al*.[35] Four micrograms of *E. coli* ArcB-enriched cytoplasmic membrane was incubated with 0.05 mM γ-[^{32}P]-ATP (37 kBq) and 4.5 μg of semi-purified PpPRR1 or PpPRR2 RLD peptide in TEG buffer (50 mM Tris–HCl, pH 8.0, 0.35 mM EDTA, 10% glycerol) containing 5 mM $MgCl_2$, 200 mM KCl and 2 mM DTT at 25°C for 1, 5 and 10 min. The reaction was terminated by the addition of SDS–PAGE sample buffer. The samples were subjected to SDS–PAGE. The gel was dried and analysed with BAS-2500.

3. Results

3.1. *Phylogenetic analyses of the moss PpPRR genes*

Previously, we identified four *PRR* homologue genes, *PpPRR1* (protein ID in the JGI *P. patens* database: 154145), *PpPRR2* (165025), *PpPRR3* (173125) and *PpPRR4* (165029) in the JGI genome database.[21] We characterized the *PpPRR1* gene (and its corresponding cDNA) as '*PpPRRa*' before,[20] but in this paper, we use the name '*PpPRR1*', not *PpPRRa*, to avoid confusion. Holm *et al*. also followed this nomenclature (*PpPRR1–PpPRR4*) deposited in the JGI genome database.[21] Other than these four sequences, we found no gene models that are significantly similar to the angiosperm *PRR* genes in the moss genome. We isolated cDNAs that cover the entire coding regions for the *PpPRR2*, *PpPRR3* and *PpPRR4* genes and confirmed that all of their predicted proteins share, as do *PpPRR1*,[20] an N-terminal RLD and a C-terminal CCT domain (Fig. 1a and b; Supplementary file 2). The receiver domains of authentic RRs share the aspartic acid–aspartic acid–lysine (DDK) motif, essential for the phosphotransfer activity,[36,37] whereas the first two residues of this motif are diverged in the angiosperm PRR proteins (Fig. 1a; for review, see Mizuno and Nakamichi[4] and Mizuno[6]). In all the available angiosperm PRR sequences, the second aspartic acid, conserved as the phosphoacceptor residue in the His–Asp phosphotransfer, is replaced by a glutamic acid (E) (Fig. 1a). In contrast, RLDs of moss PpPRR proteins are all predicted to retain the second aspartic acid; furthermore, PpPRR2, PpPRR3 and PpPRR4 also retain the first aspartic acid, hence exhibiting the complete DDK motif (Fig. 1a). PpPRR1 replaces the first aspartic acid residue with a tyrosine (Y) (Fig. 1a). These observations suggest that at least PpPRR2, PpPRR3 and PpPRR4 are potentially phosphorylated by a HK(s) as authentic RRs. The CCT domain is well conserved in all PpPRR proteins (Fig. 1b).

To examine phylogenetic relationships among *PpPRRs* and other land plant *PRRs*, we constructed a rooted phylogenetic tree using PRR homologue

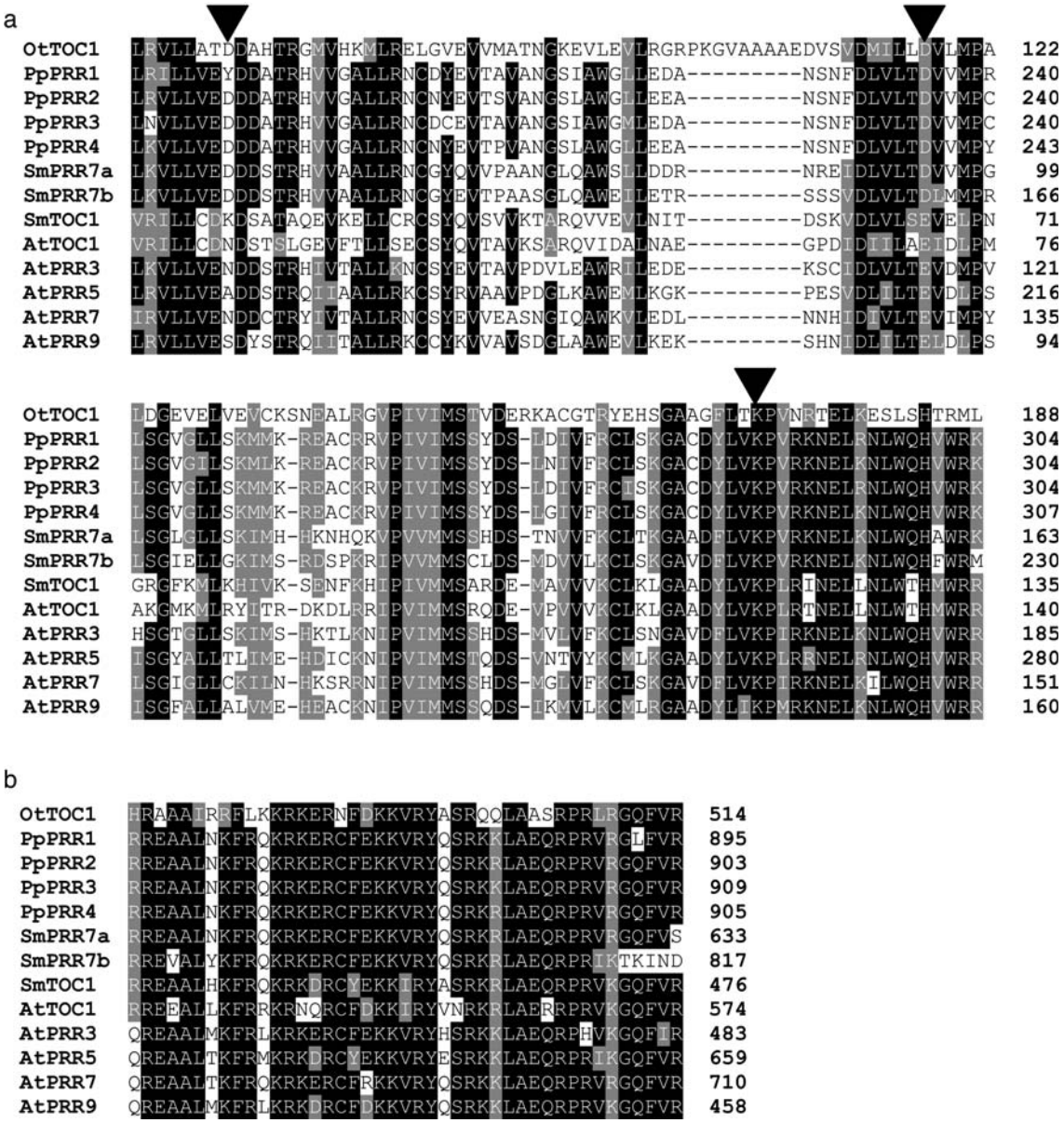

Figure 1. Alignment of conserved domains of PRR homologues from various species. RLDs (a) and CCT domains (b) of PRR homologue sequences from various plant species are aligned using ClustalW program.[26] Shading was performed using BOXSHADE ver 3.21 (http://www.ch.embnet.org/software/BOX_form.html). Amino acids identical or similar in more than 70% of the sequences are shaded by black or grey background, respectively. The number at the end of each line indicates the rightmost amino acid. Arrowheads show amino acids corresponding to the DDK motif. The PRR homologue sequences are as follows: PpPRR1, PpPRR2, PpPRR3 and PpPRR4 from *P. patens*; SmPRR7a (450934, protein ID in the JGI *Selaginella moellendorffii* database), SmPRR7b (450936), SmTOC1 (438647) from *S. moellendorffii*; OtTOC1 (AY740079 in DDBJ/EMBL/GenBank) from *O. tauri*; AtPRR3 (BAB13744), AtPRR5 (BAB13743), AtPRR7 (BAB13742) and AtPRR9 (BAB13741) from *A. thaliana*.

sequences from various plants (Fig. 2). We used the *PRR* homologue of the green alga *O. tauri* (*OtTOC1*)[16] as the outgroup because: (i) OtTOC1 is positioned relatively distant from any other PRR homologue sequences in an unrooted tree of PRRs[23]; and (ii) OtTOC1 is sister to all the other PRR homologue sequences when an authentic RR sequence is used as the outgroup (Supplementary file 3). Also included were three algal sequences: two from *C. reinhardtii* and one from *Chlorella variabilis*. In the phylogenetic tree, the angiosperm sequences are divided, as previously reported,[8,12,15] into three groups: TOC1, PRR7/3 and PRR9/5 (Fig. 2). The TOC1 group is basal to all the other sequences that include both PRR7/3 and PRR9/5 groups, indicating a more ancient origin of the TOC1 group than the other two groups. The four moss PpPRR sequences are grouped with one another, further forming a cluster with two lycophyte sequences, and this cluster is sister to the PRR7/3 group (Fig. 2). This indicates

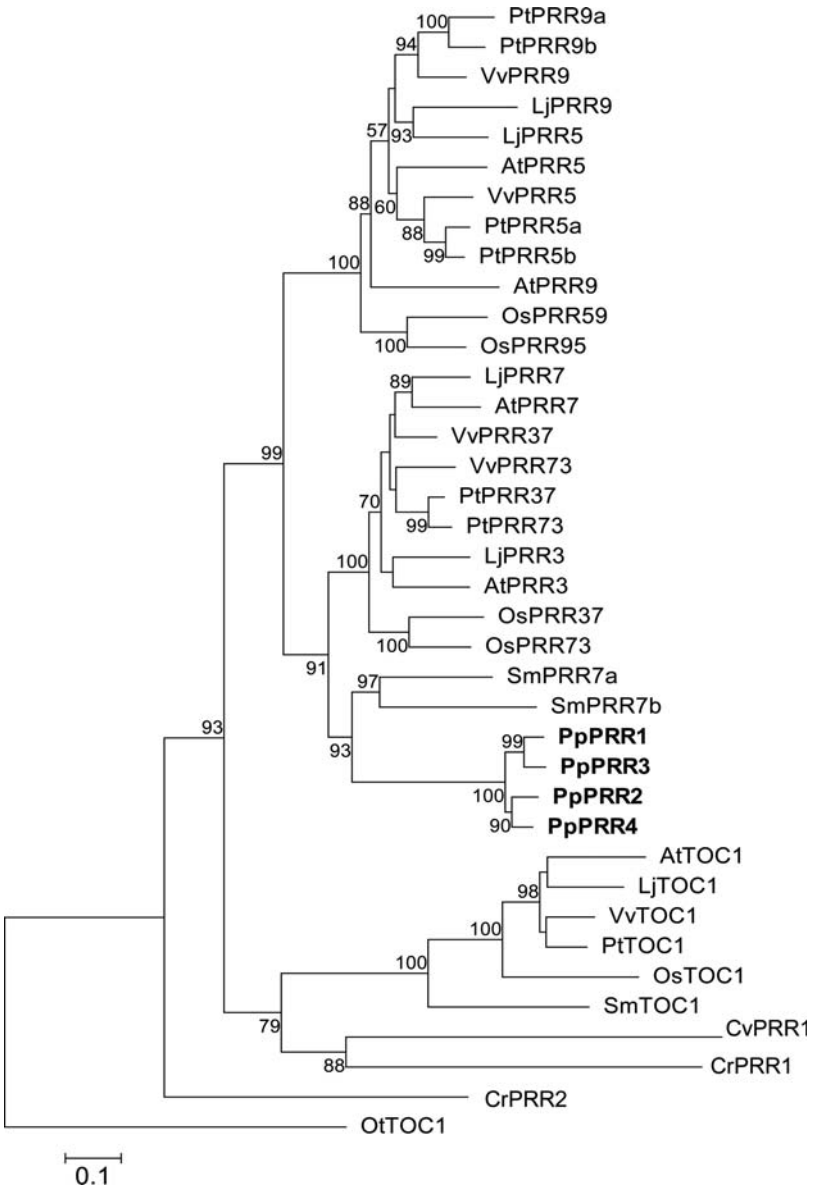

Figure 2. Phylogenetic tree of PRR homologues in various plants. Amino acid sequences of PRR homologues including entire RLD and CCT domain regions were aligned using ClustalW program and the phylogenetic tree was reconstructed by the ME method[28] by using MEGA4.1.[30] The *O. tauri* PRR homologue (OtTOC1[16]) was used as the outgroup. The numbers at each node represent the bootstrap values calculated based on 1000 bootstrap sampling and those that are higher than 50% are shown. The three PRR subfamilies are indicated. PpPRRs from *P. patens* are indicated in bold. Sequences used are as follows: OsTOC1 (BAD38854 in DDBJ/EMBL/GenBank), OsPRR37 (BAD38855), OsPRR73 (BAD38856), OsPRR59 (AK120059) and OsPRR95 (BAD38857) from *Oryza sativa*; PtTOC1 (XP_002330130.1 in NCBI protein database), PtPRR37 (XP_002311123.1), PtPRR73 (XP_002316333.1), PtPRR5a (XP_002321349.1), PtPRR5b (XP_002301442.1), PtPRR9a (XP_002320232.1) and PtPRR9b (XP_002301443.1) from *Populus trichocarpa*; VvTOC1 (XP_002281757.1), VvPRR37 (XP_002281776), VvPRR73 (XP_002275645), VvPRR5 (XP_002270811) and VvPRR9 (XP_002266192.1) from *Vitis vinifera*; LjTOC1 (chr4.CM0087.600.nc in miyakogusa.jp; http://www.kazusa.or.jp/lotus/index.html), LjPRR3 (LjT08O17.180/130/120), LjPRR5 (chr1.CM0105.560), LjPRR7 (chr3.LjT05P05.60) and LjPRR9 (chr3.CM0208.230) from *Lotus japonicas*;[42] CrPRR1 (XP_001695777.1), CrPRR2 (XP_001701808.1) from *Chlamydomonas reinhardtii*; CvPRR1 (EFN58892.1) from *C. variabilis*. For other sequences, refer to the legend for Fig. 1.

that the moss *PpPRR* genes are more closely related to the PRR7/3 group than to the two other groups. The four moss sequences are divided into two groups PpPRR1/PpPRR3 and PpPRR2/PpPRR4 (Fig. 2).

Next, we compared the distribution of intron insertion sites on the RLD and CCT coding regions between *PRR* genes (Fig. 3). In the RLD region, two insertion sites are conserved among all the *PRR* sequences examined (Fig. 3a; see Takata *et al.*[15]). This distribution pattern of intron insertion sites is clearly different from those seen in the receiver domain of authentic RRs,[13] confirming the idea that *PRR* genes

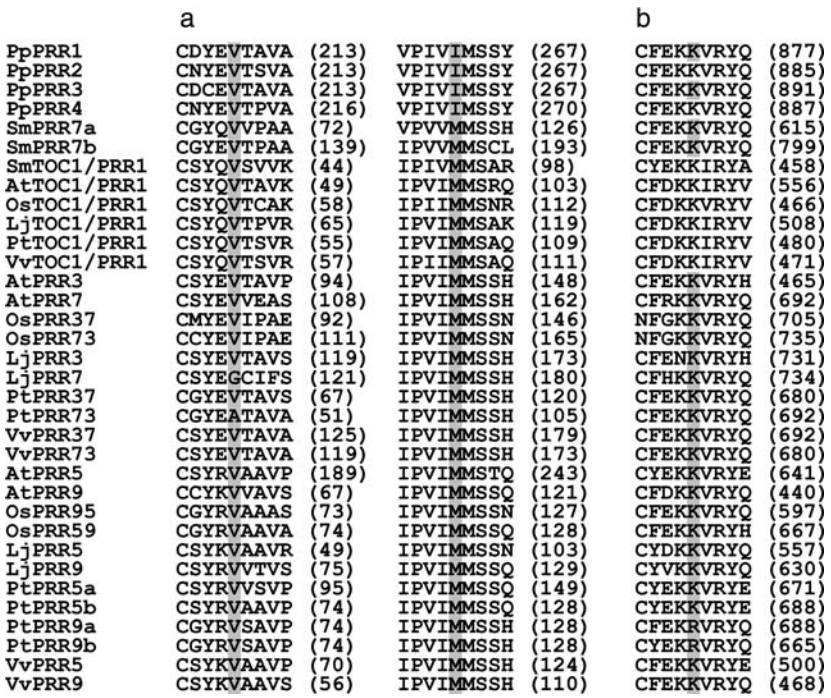

Figure 3. Distribution of intron insertion sites on the conserved domains of PRR sequences. From the aligned amino acid sequences of PRR proteins, only three stretches [two from RLD (a) and one from CCT (b)] are shown, each consisting of nine amino acids with the amino acid corresponding to an intron insertion site (shaded in grey) being centred. The number of the rightmost amino acid of each stretch is indicated in parentheses. For the sequences used, refer to the legend of Fig. 2.

diverged distinctly from authentic *RR* genes. In the CCT domain region, the TOC1 group sequences are unique in that they show no intron, whereas all sequences in the other two groups have a conserved single insertion site in the middle of the domain (Fig. 3b; see Takata *et al.*[15]). *PpPRR* sequences are divided into two groups, *PpPRR1/PpPRR3* with one intron (like the PRR7/3 and PRR9/5 groups) and *PpPRR2/PpPRR4* with no intron (like the TOC1 group; Fig. 3). This divergence is consistent with the results of the phylogenetic tree (Fig. 2), whereas the loss of an intron in *PpPRR2/PpPRR4* should have occurred in the moss lineage independently from the TOC1 group (Fig. 2).

3.2. In vitro *phosphotransfer from a HK to the RLD of PpPRR2*

We examined whether RLDs of PpPRR1 and PpPRR2, both of which retain the potential phosphoacceptor residue while showing mutually diverged features (Figs 1–3), are phosphorylated by a His–Asp phosphorelay process in an *in vitro* phosphotransfer assay (Fig. 4). In this assay, ArcB, an *E. coli* HK, added in excess and hence lacking substrate specificity, transfers its phosphate to the phosphoacceptor site in a receiver domain. We purified the RLD peptides of PpPRR1 and PpPRR2 overexpressed in *E. coli* cells (Fig. 4b and c) and tested each of them to assess whether or not they undergo phosphotransfer. The PpPRR2 RLD peptide was phosphorylated within 5 min in the presence of ArcB (Fig. 4g). The phosphorylation levels of ArcB decreased concomitantly (Fig. 4g), indicating that the phosphorylation of PpPRR2 RLD is due to phosphotransfer from ArcB. On the other hand, we could not detect any phosphorylation signal with PpPRR1 RLD (Fig. 4f), consistent with its relatively diverged RLD sequence (Fig. 1a). When the PpPRR2 RLD peptide was incubated with the membrane fraction with no overexpressed ArcB, we could not detect the phosphorylation signal (Fig. 4h). This supports the interpretation that the increased levels of phosphorylation seen with the PpPRR2 RLD peptide (Fig. 4g) is due to phosphotransfer from ArcB, but not due to other types of kinases. These observations indicate that PpPRR2 presumably functions as an RR in an unknown His–Asp phosphorelay signal transduction pathway in *P. patens*. Moreover, PpPRRs likely diverged from one another based not only on their RLD sequences but also on their phosphotransfer ability.

3.3. *Circadian regulation of PpPRR expression profiles*

In a previous study,[20] we reported that the *PpPRR1* mRNA accumulation showed circadian variation in 12-h light and 12-h dark cycles (12:12LD) and in continuous darkness (DD), but not in continuous

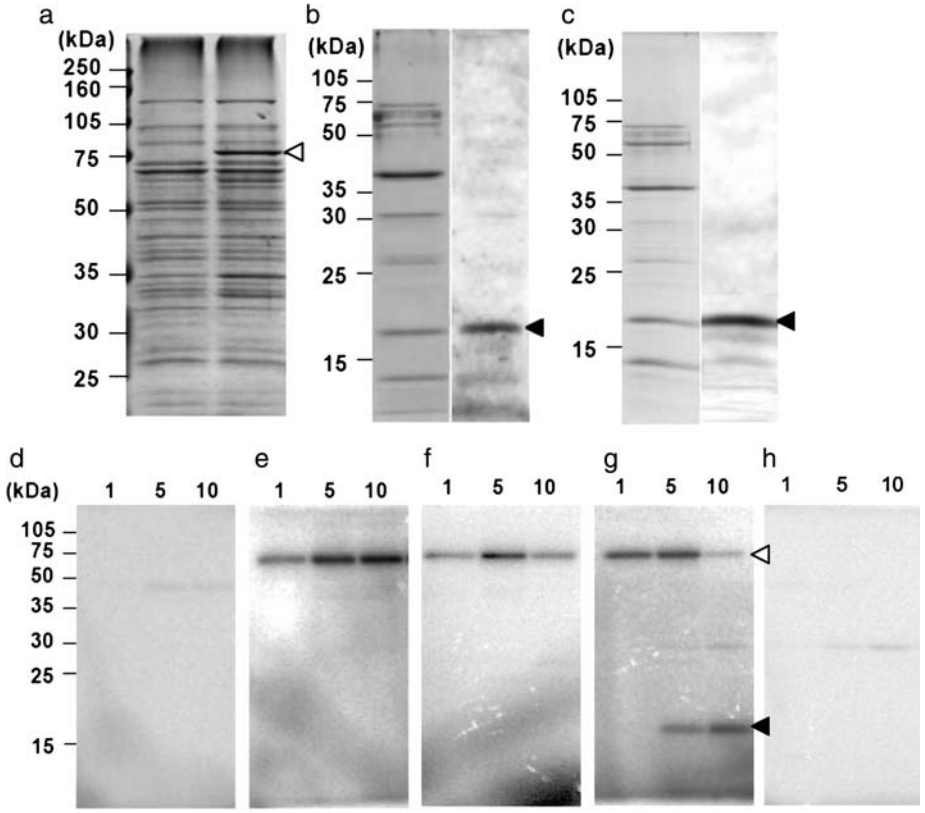

Figure 4. *In vitro* His–Asp phosphotransfer to the PpPRR2 RLD peptide. (a) Overproduction of ArcB in *E. coli* cells. The cytoplasmic membrane proteins were extracted from an ArcB overproducer (right lane) and a negative control strain of *E. coli* (left lane), subjected to SDS–PAGE and detected with Coomassie Brilliant Blue (C.B.B.) (see 2.7. Preparation of the E. coli ArcB-enriched cytoplasmic membrane). The ArcB band of around 88 kDa is indicated with an open triangle. Purification of PpPRR1 (b) and PpPRR2 RLD (c) peptides is shown. PpPRR1 and PpPRR2 RLD peptides were, respectively, affinity purified with TALON^{TM} metal affinity resin from the soluble protein fraction of cell lysate of each overproducer strain, subjected to SDS–PAGE and detected with C.B.B. Existence of PpPRR1 and PpPRR2 RLD peptides were further confirmed by western blotting with anti-6×His antibodies; PpPRR1 and PpPRR2 RLD peptides (~17 kDa for each) are indicated with closed triangles. (d and e) Results of autophosphorylation assay. *Escherichia coli* ArcB-enriched membranes (e) or control membranes (d) were incubated with γ-[^{32}P]-ATP for indicated times. (f–h) Results of *in vitro* His–Asp phosphotransfer assay. *Escherichia coli* ArcB-enriched membranes were incubated with γ-[^{32}P]-ATP for indicated times in the presence of PpPRR1 (f) or PpPRR2 (g) RLD peptide. A reference reaction was conducted using control membranes incubated with γ-[^{32}P]-ATP for indicated times in the presence of PpPRR2 RLD peptide (h). Signals from the gels were analysed by BAS-2500 for their phosphorylation status.

light (LL), by conducting sqRT-PCR analysis. Here, we studied mRNA accumulation profiles for all four *PpPRR* genes with the same method (Fig. 5). In 12:12LD, all genes showed high-amplitude mRNA rhythms with a period of ~1 day, which peaked in the latter half of the light phase (Fig. 5a). In DD, all genes showed endogenous rhythms with damping (Fig. 5b). These rhythms in 12:12LD or DD showed phase relationships roughly similar to *A. thaliana PRR3*, *PRR5* or *PRR7* genes.[4,6] In LL, in contrast, all the genes exhibited no hint of circadian regulation and were arrhythmic as demonstrated for *PpPRR1* (Fig. 5c; see Okada *et al.*[20]). The arrhythmic profiles in LL are consistent with our observations that the moss genes so far tested are, if clock gene homologues or clock-controlled genes, all arrhythmic in LL,[38–40] and this is in contrast to angiosperm *PRR* genes, all of which show robust circadian rhythms in LL.[4,6]

The results of the sqRT-PCR experiments suggest that phases of the four genes seem to be differentially fine-tuned into two types: in 12:12LD, troughs of *PpPRR1/PpPRR3* occurred 4 h before dawn, whereas those of *PpPRR2/PpPRR4* just at dawn (Fig. 5a). We also measured mRNA accumulation for *PpPRRs* in one cycle of 12:12LD by the qRT-PCR analysis with a shorter sampling interval (Fig. 6). At ZT01 (ZT, zeitgeber time: time in a light–dark cycle, putting the light onset as ZT0), the levels of *PpPRR1/PpPRR3* showed certain increase (30–40% of the maximum levels), whereas those of *PpPRR2/PpPRR4* were still very close to zero (Fig. 6), confirming the distinction of expression profiles between *PpPRR1/PpPRR3* and *PpPRR2/PpPRR4*. This differential fine-tuning appears to be conferred by the endogenous circadian clock, because the sampling of cells at dawn (Fig. 5a, hours 0 and 24)

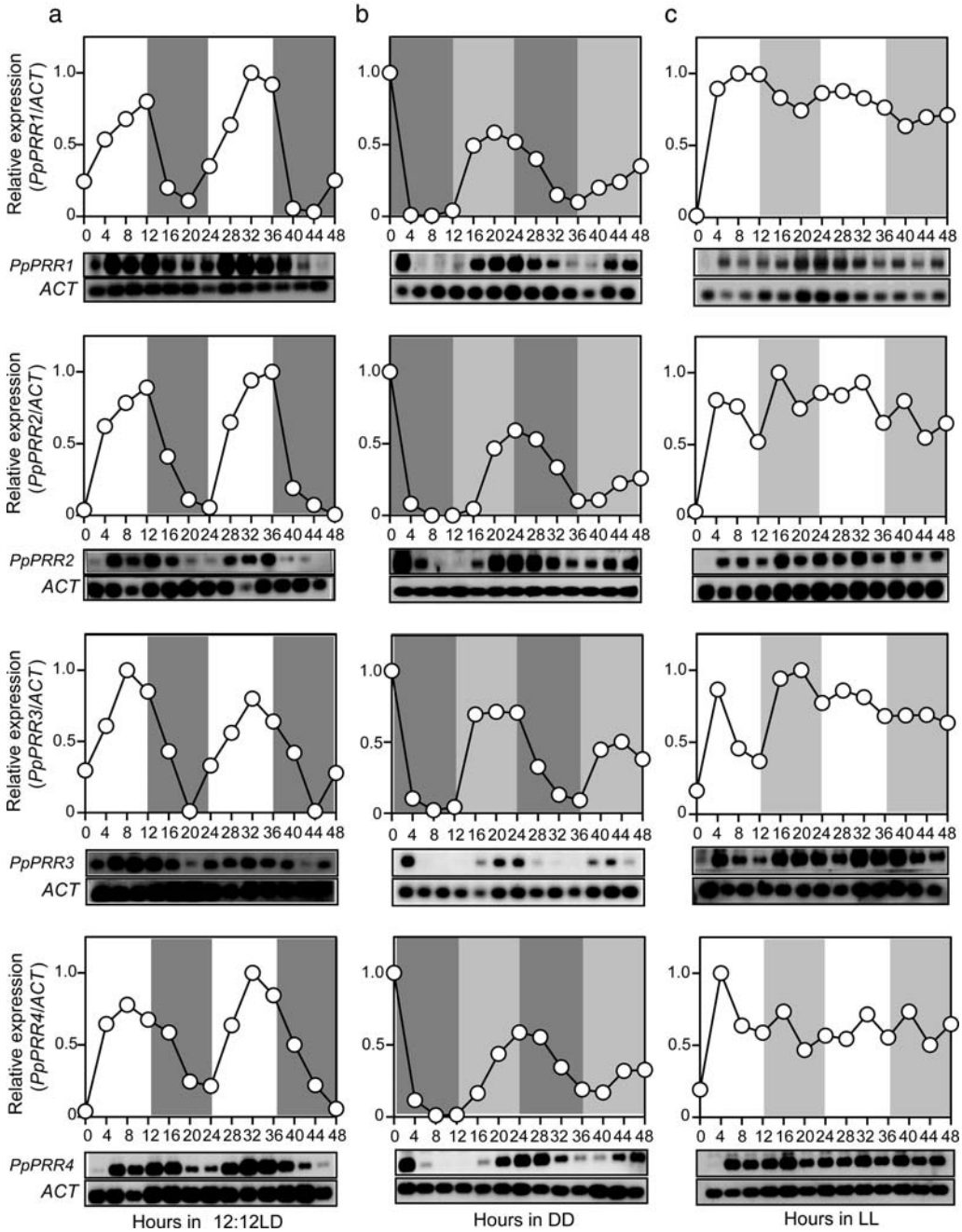

Figure 5. Changes in mRNA abundance for the *PpPRR* genes under 12:12LD, DD and LL conditions examined by the sqRT-PCR analysis. *Physcomitrella patens* protonemal cells were maintained in 12:12LD for more than 2 weeks after which cells were harvested in 12:12LD (a), DD (b) or LL (c) conditions at indicated times. From the top, changes in mRNA abundance for *PpPRR1*, *PpPRR2*, *PpPRR3* and *PpPRR4* are shown. Light conditions are overlaid with each graph: regions with no shade and those shaded with dark grey represent light and dark phases, respectively; regions shaded with light grey represent subjective light phases in (b) or subjective dark phases in (c). Graphs show the results of quantification of the mRNA levels for each gene after normalization to those for actin as a control.[39] The maximum levels are set to 1.0. The photo below each graph shows the hybridized bands for each test gene or the control *actin* gene, detected as chemiluminescence signals. We obtained similar results in two independent experiments.

was performed in the absence of light. This idea is also supported by the rhythms of *PpPRRs* in DD, where endogenous clock regulation is more clearly seen: the first peaks of *PpPRR2*/*PpPRR4* lagged behind those of *PpPRR1*/*PpPRR3* by around 4 h (Fig. 5b; Supplementary file 4).

3.4. *Induction of PpPRR by light*

We examined the effect of light on the accumulation of the *PpPRR* mRNAs by sqRT-PCR analyses. The mRNAs of all four *PpPRRs* were induced by a 2-h pulse of white, blue or red light (Fig. 7). The rates of induction by white light are 8.7 for *PpPRR1*, 2.6 for

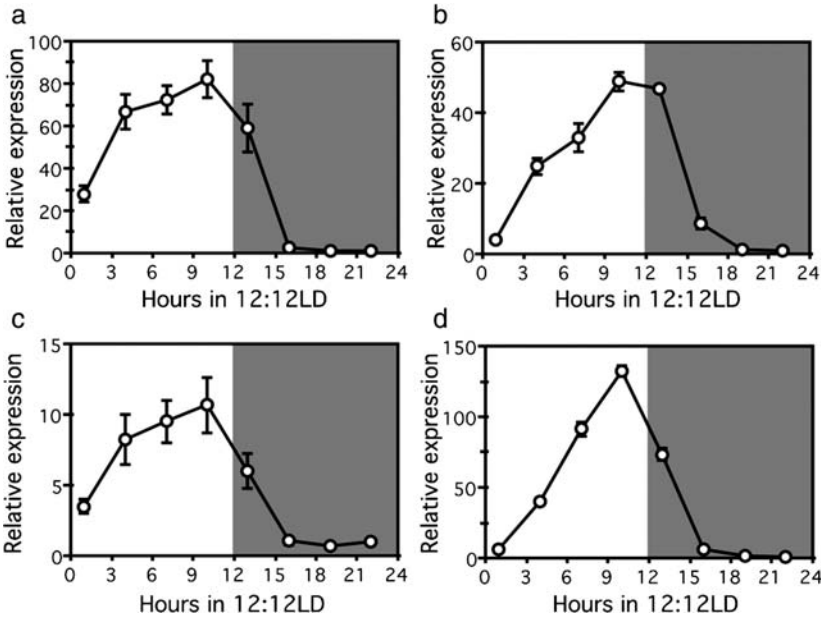

Figure 6. Changes in mRNA abundance for the *PpPRR* genes for one 12:12LD cycle examined by the qRT-PCR analysis. *Physcomitrella patens* protonemal cells were maintained in 12:12LD for more than 2 weeks after which cells were harvested in one full cycle of 12:12LD at indicated times. Shown are the changes in mRNA abundance for *PpPRR1* (a), *PpPRR2* (b), *PpPRR3* (c) and *PpPRR4* (d). Light conditions are overlaid with each graph: regions with no shade and those shaded with dark grey represent light and dark phases, respectively. The graphs show the averages and the standard deviations of four independent experiments, in which the results of quantification of mRNA levels for each gene were normalized to those of *actin* as a control.[39]

PpPRR2, 6.2 for *PpPRR3* and 2.5 for *PpPRR4*. The rates of induction for *PpPRR1* and *PpPRR3* are the highest and second highest, respectively, for any colour of light; this observation does not contradict the idea that there is an intraspecific divergence between *PpPRR1/PpPRR3* and *PpPRR2/PpPRR4*. The rates of induction by blue light and red light are lower than those of white light for any *PpPRR* gene.

4. Discussion

The results of the current study help to understand the origins of the angiosperm *PRR* genes. In our *in vitro* assay, the PpPRR2 RLD peptide underwent phosphotransfer (Fig. 4), consistent with its complete DDK motif (Fig. 1a), strongly suggesting that PpPRR2 functions as an RR. Besides, according to our phylogenetic tree (Fig. 2), PpPRRs are phylogenetically closely related to angiosperm PRRs. Therefore, it is presumed that the similarity of RLDs of PRRs to the authentic receiver domain is not only superficial but that PRRs were certainly derived from an authentic RR. Most probably, angiosperm PRRs have lost their phosphorelay function through the course of evolution, largely due to the substitution of the phosphoacceptor aspartic acid to a glutamic acid in their RLDs, and other critical residues such as the first aspartic acid of the DDK motif should have concomitantly diverged. Importantly, the *O. tauri* OtTOC1 and the *C. reinhardtii* CrPRR2 also share not only the potential phosphoacceptor aspartic acid but also the entire DDK motif (Fig. 1a; see Corellou *et al.*[16]). Although there has so far been no report about whether or not these algal proteins undergo phosphotransfer, they are also assumed to function as RRs, representing prototypic proteins of the land plant PRRs.

Our results also offer evolutionary explanations not only for the origin but also for the diversity of *PRRs* in land plants (Fig. 8). The pattern of our tree indicates that the TOC1 group first diverged, and then split the PRR9/5 group and the other branch, the latter containing the PRR7/3 group. Since PpPRRs are positioned inside the branch containing the PRR7/3 group, the origins of the TOC1 and PRR9/5 groups date back before the divergence of moss from higher plant lineages. The ancient origin of the TOC1 group is supported by the observation that *C. reinhardtii* and *C. variabilis* seem to have a TOC1 ortholog (Fig. 2). Furthermore, since the cluster of PpPRRs and lycophyte SmPRR7a/7b is sister to all the angiosperm PRR7/3 sequences (Fig. 2), the divergence between the PRR7/3 group and the ancestor of PpPRRs and SmPRR7a/7b also predate the divergence of moss from higher plants. Therefore, the common ancestor of moss and higher plants possessed *TOC1*, *PRR7/3* and *PRR9/5* orthologues in its genome, but these genes appear to have been lost later within the moss lineage (Fig. 8). In the lycophyte lineage, *PRR7/3* and *PRR9/5* orthologues have been lost and

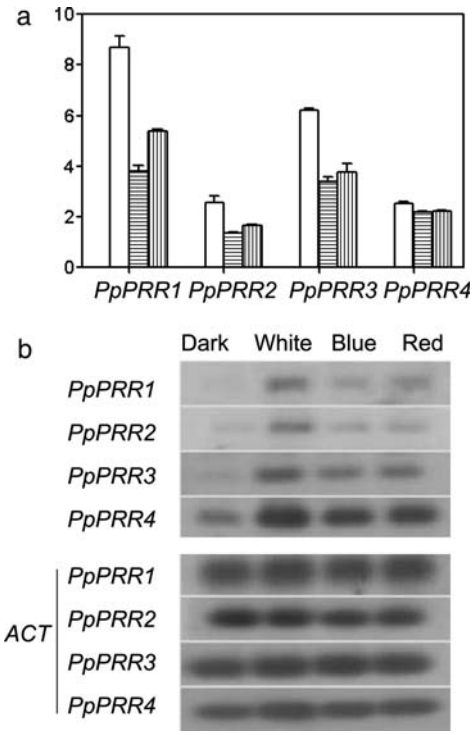

Figure 7. Light-induced expression of the *PpPRR* genes examined by the sqRT-PCR analysis. *Physcomitrella patens* protonemal cells were maintained under LL for 1 week, exposed to darkness for 24 h, and 2 h of white light, blue light, red light or dark period was administered before the cells were sampled. The fluence rate of each colour or light was 40 μmol m^{-2} s^{-1}. Total RNAs were extracted, and the abundances of *PpPRR* mRNAs were measured and normalized to those for *actin* as a control. The graph shows the mRNA levels of *PpPRRs* induced by different colour of light (white light, open bars; blue light, bars with horizontal hatches; red light, bars with vertical hatches) relative to those from samples maintained in the prolonged darkness, the latter of which are set to 1.0. Values are the mean $\pm$ SD of three replications. The bottom photos show the hybridized bands for *PpPRRs* (upper four slips) or the control *actin* gene for each *PpPRR* (lower four slips), detected as chemiluminescence signals. We obtained similar results in two independent experiments.

the unique combination of the *TOC1* (*SmTOC1*) and *PpPRR* (*SmPRR7a/7b*) orthologues still now remain (Fig. 8). In the angiosperm lineage, only *PpPRR* ortholog(s) has been lost, resulting in the current three *PRR* groups (Fig. 8). Concerning the timings of substitution of the phosphoacceptor residue, there are two alternative explanations. In one scenario (Fig. 8a), the phosphoacceptor aspartic acid residue of the PpPRRs and SmPRR7a/7b can be traced back to that found in the algal sequences; the phosphoacceptor residue in these sequences has never been substituted. This explanation might seem simple and more likely; however, if this were the case, the aspartic acid residue must have been substituted, according to the branching patterns of our tree, independently within each lineage of the TOC1, PRR7/3 and PRR9/5 groups (Figs 2 and 8a). In another scenario (Fig. 8b), simpler at least in terms of the frequency of substitutions, the aspartic acid was substituted only once to a glutamic acid before the divergence of all the land plant PRR subfamilies. In this case, an aspartic acid was regained by a second substitution in the ancestral lineage of *PpPRRs* and two lycophyte genes (Fig. 8b). If this were the case, *PpPRR1* might be, again, in the process of divergence from authentic RR-type sequences. In order to know which hypothesis, or yet another scenario, is more plausible, we need more sequence data; in particular, *PRR* sequences should be characterized from other primitive plants, i.e. liverworts, hornworts, ferns and gymnosperms.

Our results demonstrate intraspecific divergences among the *PpPRR* genes. The phylogenetic tree (Fig. 2), intron insertion sites (Fig. 3) and expression profiles (Figs 5–7 and Supplementary file 4) suggest the divergence between *PpPRR1/PpPRR3* and *PpPRR2/PpPRR4*. The *A. thaliana PRR* family members show differentially regulated expression profiles, reflecting the fact that they act at different nodes in the circadian network and functionally diverged from one another.[4,6] Therefore, *PpPRR1/PpPRR3* and *PpPRR2/PpPRR4* are also predicted to be functionally diverged. It should be noted that Holm *et al.*[23] did not detect any differential expression among the four genes in a light–dark cycle followed by DD. This may be because their light–dark regime is different from ours: they used a long day regime, a 16-h light and 8-h dark cycle, whereas ours is a 12-h light and 12-h dark cycle(s) (12:12LD; Figs 5 and 6). All *PpPRRs* are induced by light (Fig. 7), and this light responsiveness may have apparently synchronized the trough phases of *PpPRRs* with the earlier dawn in the short night of their long day regime, whereas difference in trough phases between *PpPRR1/PpPRR3* and *PpPRR2/PpPRR4* are obvious in our longer nights (Fig. 5a).

On the other hand, the results of the *in vitro* assay (Fig. 4) and detailed sequence comparison (Fig. 1a) suggest that PpPRR2/PpPRR3/PpPRR4 function as RRs, whereas PpPRR1 does not or its phosphotransfer ability is very weak. The moss PpPRRs, if not all of them, are anticipated to have some clock-associated functions as do *A. thaliana* PRRs, from the following facts: (i) the circadian networks of *A. thaliana* and *P. patens* are predicted to be at least partially conserved[20]; and (ii) *O. tauri*, which belongs to green algae, the closest relative of land plants, has a *PRR* homologue that functions as a clock gene.[16] Since RRs are generally involved in signalling cascades responsive to environmental/endogenous signals, PpPRR2/PpPRR3/PpPRR4 might function, rather than in the core clock circuitry, in an input pathway(s) that must be responsive to environmental cues such as light and temperature.

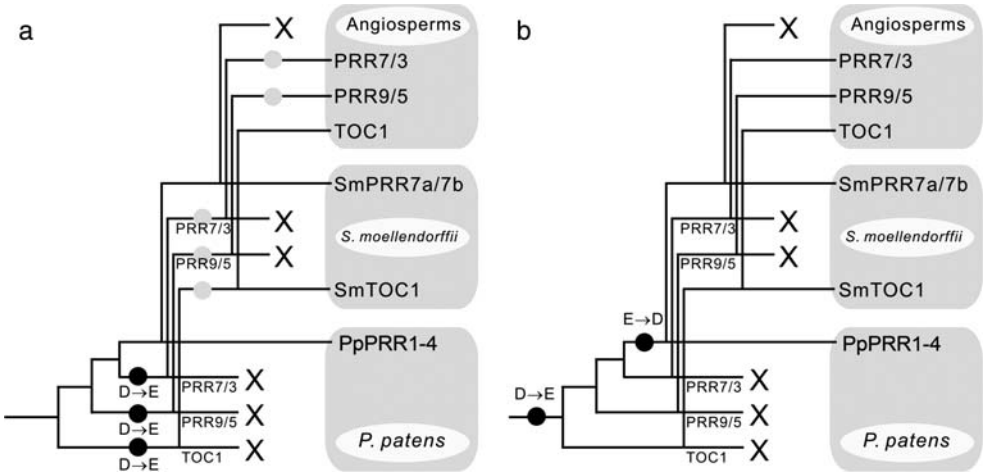

Figure 8. Evolutionary scenarios for divergence of *PpPRR* genes in land plants. Two alternative explanations are presented: (a) scenario in which the phosphoacceptor aspartic acid residue in PpPRR and SmPRR7a/7b sequences has never been substituted and (b) scenario in which the aspartic acid was substituted to glutamic acid only once and it was regained by a second substitution in the ancestral lineage of *PpPRRs* and two lycophyte genes. Closed circles represent amino acid substitution events at the potential phosphoacceptor residue. Grey circles represent alternative timings of amino acid substitutions indicated by the closed circles. Crosses represent gene loss events (see the main text for detailed description).

In a future study, in parallel with gene knock out experiments, it should also be addressed whether PpPRRs are involved in phosphotransfer functions *in planta*. Moreover, a HK(s) and a HPt(s) that are partners to (at least some of) PpPRR proteins should be characterized. It might not be easy to identify a partner HK(s) because the *P. patens* genome contains as many as ~50 HK sequences,[22] unlike *A. thaliana*, which contains only 8 HK genes.[41] However, the availability of the entire genome sequence, many full-length cDNA clones and the tractability of gene functional analysis based on gene targeting techniques will support the identification of such HK and HPt genes in *P. patens*, possibly as novel clock genes.

4.1. Conclusion

Here, we demonstrated that the moss PpPRRs have close relationships with angiosperm PRRs and at least PpPRR2 can function as an RR, indicating that the plant clock-associated *PRR* families are derived from an authentic RR(s). Moreover, here, we offered evolutionary explanations for divergence of *PRR* genes in land plants. This study should be a foundation for understanding how a particular set of genes involved in regulation of the clock evolved their functions, in coordination with changes (or maintenance) of the clock mechanisms.

4.2. Accession numbers for the sequence data

The sequences reported in this paper have been submitted to the public databases [DDBJ/EMBL/GenBank: AB558266 (*PpPRR1*), AB558268 (*PpPRR2*), AB558267 (*PpPRR3*) and AB558269 (*PpPRR4*)].

Supplementary Data: Supplementary data are available at www.dnaresearch.oxfordjournals.org.

Acknowledgements: We thank Yuichi Oba (Nagoya University) and Kyoko Kanamaru (Nagoya University) for valuable advice and helpful discussion. We also thank Mayu Nakagawa (Nagoya University) and K. Sreenath (University of Massachusetts Medical School) for critical reading of the manuscript and Andrew Millar (Department of Biological Science, University of Edinburgh) for the BRASS software package.

Funding

This study was supported by grants from the Ministry of Education, Culture, Sports, Science and Technology Japan (MEXT) to S.B.S. and from the Japan Society for the Promotion of Science (JSPS) (21570005 to S.A. and 21780092 to T.Y.).

References

1. Edmunds, L.N. 1988, *Cellular and Molecular Bases of Biological Clocks*, Springer: New York.
2. Pittendrigh, C.S. 1993, Temporal organization: reflections of a Darwinian clock-watcher, *Annu. Rev. Physiol.*, **55**, 16–54.
3. Hamilton, E.E. and Kay, S.A. 2008, SnapShot: circadian clock proteins, *Cell*, **135**, 368–8.
4. Mizuno, T. and Nakamichi, N. 2005, Pseudo-response regulators (PRRs) or true oscillator components (TOCs), *Plant Cell Physiol.*, **46**, 677–85.
5. Harmer, S.L. 2009, The circadian system in higher plants, *Annu. Rev. Plant Biol.*, **60**, 357–77.

6. Mizuno, T. 2005, Two-component phosphorelay signal transduction systems in plants: from hormone responses to circadian rhythms, *Biosci. Biotechnol. Biochem.*, **69**, 2263–76.
7. Makino, S., Kiba, T., Imamura, A., et al. 2000, Genes encoding pseudo-response regulators: insight into His-to-Asp phosphorelay and circadian rhythm in *Arabidopsis thaliana*, *Plant Cell Physiol.*, **41**, 791–803.
8. Murakami, M., Ashikari, M., Miura, K., Yamashino, T. and Mizuno, T. 2003, The evolutionarily conserved *OsPRR* quintet: rice pseudo-response regulators implicated in circadian rhythm, *Plant Cell Physiol.*, **44**, 1229–36.
9. Hecht, V., Foucher, F., Ferrándiz, C., et al. 2005, Conservation of *Arabidopsis* flowering genes in model legumes, *Plant Physiol.*, **137**, 1420–34.
10. Hecht, V., Knowles, C.L., Vander Schoor, J.K., et al. 2007, Pea *LATE BLOOMER1* is a *GIGANTEA* ortholog with roles in photoperiodic flowering, deetiolation, and transcriptional regulation of circadian clock gene homologs, *Plant Physiol.*, **144**, 648–61.
11. Ramos, A., Pérez-Solís, E., Ibáñez, C., et al. 2005, Winter disruption of the circadian clock in chestnut, *Proc. Natl Acad. Sci. USA*, **102**, 7037–42.
12. Miwa, K., Serikawa, M., Suzuki, S., Kondo, T. and Oyama, T. 2005, Conserved expression profiles of circadian clock-related genes in two *Lemna* species showing long-day and short-day photoperiodic flowering responses, *Plant Cell Physiol.*, **47**, 601–12.
13. Ishida, K., Yamashino, T., Yokoyama, A. and Mizuno, T. 2008, Three type-B response regulators, ARR1, ARR10 and ARR12, play essential but redundant roles in cytokinin signal transduction throughout the life cycle of *Arabidopsis thaliana*, *Plant Cell Physiol.*, **49**, 47–57.
14. Liu, H., Wang, H., Gao, P., et al. 2009, Analysis of clock gene homologs using unifoliolates as target organs in soybean (*Glycine max*), *J. Plant Physiol.*, **166**, 278–89.
15. Takata, N., Saito, S., Satio, C.T. and Uemura, M. 2010, Phylogenetic footprint of the plant clock system in angiosperms: evolutionary processes of pseudo-response regulators, *BMC Evol. Biol.*, **10**, 126.
16. Corellou, F., Schwartz, C., Motta, J.P., Djouani-Tahri el, B., Sanchez, F. and Bouget, F.Y. 2009, Clocks in the green lineage: comparative functional analysis of the circadian architecture of the picoeukaryote *Ostreococcus*, *Plant Cell*, **21**, 3436–49.
17. Bowman, J.L., Floyd, S.K. and Sakakibara, K. 2007, Green genes-comparative genomics of the green branch of life, *Cell*, **129**, 229–34.
18. Lang, D., Zimmer, A.D., Rensing, S.A. and Reski, R. 2008, Exploring plant biodiversity: the *Physcomitrella* genome and beyond, *Trends Plant Sci.*, **13**, 542–9.
19. Schaefer, D.G. and Zrÿd, J.P. 1997, Efficient gene targeting in the moss *Physcomitrella patens*, *Plant J.*, **11**, 1195–206.
20. Okada, R., Kondo, S., Satbhai, S.B., Yamaguchi, N., Tsukuda, M. and Aoki, S. 2009, Functional characterization of *CCA1/LHY* homolog genes, *PpCCA1a* and *PpCCA1b*, in the moss *Physcomitrella patens*, *Plant J.*, **60**, 551–63.
21. DOE Joint Genome Institute. *P. patens* subsp *patens* V1.1, http://genome.jgi-psf.org//Phypa1_1/Phypa1_1.home.html.
22. Rensing, S.A., Lang, D., Zimmer, A.D., et al. 2010, The *Physcomitrella* genome reveals evolutionary insights into the conquest of land by plants, *Science*, **319**, 64–9.
23. Holm, K., Källman, T., Gyllenstrand, N., Hedman, H. and Lagercrantz, U. 2010, Does the core circadian clock in the moss *Physcomitrella patens* (Bryophyta) comprise a single loop? *BMC Plant Biol.*, **10**, 109.
24. Ashton, N.W. and Cove, D.J. 1977, The isolation and preliminary characterization of auxotrophic and analogue resistant mutants in the moss *Physcomitrella patens*, *Mol. Gen. Genet.*, **154**, 87–95.
25. Nishiyama, T., Hiwatashi, Y., Sakakibara, I., Kato, M. and Hasebe, M. 2000, Tagged mutagenesis and gene-trap in the moss, *Physcomitrella patens* by shuttle mutagenesis, *DNA Res.*, **7**, 9–17.
26. Higgins, D.G. and Sharp, P.M. 1988, CLUSTAL: a package for performing multiple sequence alignment on a microcomputer, *Gene*, **73**, 237–44.
27. Jones, D.T., Taylor, W.R. and Thornton, J.M. 1992, The rapid generation of mutation data matrices from protein sequences, *Comput. Appl. Biosci.*, **8**, 275–82.
28. Rzhetsky, A. and Nei, M. 1992, A simple method for estimating and testing minimum evolution trees, *Mol. Biol. Evol.*, **9**, 945–67.
29. Felsenstein, J. 1985, Confidence limits on phylogenies: an approach using the bootstrap, *Evolution*, **39**, 783–91.
30. Tamura, K., Dudley, J., Nei, M. and Kumar, S. 2007, MEGA4: Molecular Evolutionary Genetics Analysis (MEGA) software version 4.0, *Mol. Biol. Evol.*, **24**, 1596–9.
31. Guindon, S., Lethiec, F., Duroux, P. and Gascuel, O. 2005, PHYML Online–a web server for fast maximum likelihood-based phylogenetic inference, *Nucleic Acids Res.*, **33**, W557–9.
32. Nakamichi, N., Kita, M., Niinuma, K., Ito, S., Yamashino, T., Mizoguchi, T. and Mizuno, T. 2007, *Arabidopsis* clock-associated pseudo-response regulators PRR9, PRR7 and PRR5 coordinately and positively regulate flowering time through the canonical CONSTANS-dependent photoperiodic pathway, *Plant Cell Physiol.*, **48**, 822–32.
33. Lowry, O.H., Rosebrough, N.J., Farr, A.L. and Randall, R.J. 1951, Protein measurement with the Folin phenol reagent, *J. Biol. Chem.*, **193**, 265–75.
34. Tsuzuki, M., Ishige, K. and Mizuno, T. 1995, Phosphotransfer circuitry of the putative multi-signal transducer, ArcB, of *Escherichia coli*: *in vitro* studies with mutants, *Mol. Microbiol.*, **18**, 953–62.
35. Azuma, N., Kanamaru, K., Matsushika, A., Yamashino, T., Mizuno, T., Kato, M. and Kobayashi, T. 2007, *In vitro* analysis of His-Asp phosphorelays in *Aspergillus nidulans*: the first direct biochemical evidence for the existence of His-Asp phosphotransfer systems in filamentous fungi, *Biosci. Biotechnol. Biochem.*, **71**, 2493–502.
36. Parkinson, J.S. and Kofoid, E.C. 1992, Communication modules in bacterial signaling proteins, *Ann. Rev. Genet.*, **26**, 71–112.
37. Ueguchi, C., Koizumi, H., Suzuki, T. and Mizuno, T. 2001, Novel family of sensor histidine kinase genes in *Arabidopsis thaliana*, *Plant Cell Physiol.*, **42**, 231–5.

38. Aoki, S., Kato, S., Ichikawa, K. and Shimizu, M. 2004, Circadian expression of the *PpLhcb2* gene encoding a major light-harvesting chlorophyll a/b-binding protein in the moss *Physcomitrella patens*, *Plant Cell Physiol.*, **45**, 68–76.
39. Ichikawa, K., Sugita, M., Imaizumi, T., Wada, M. and Aoki, S. 2004, Differential expression on a daily basis of plastid sigma factor *PpSig* genes from the moss *Physcomitrella patens*: regulatory interactions among *PpSig5*, the circadian clock and blue light signaling mediated by cryptochromes, *Plant Physiol.*, **136**, 4285–98.
40. Shimizu, M., Ichikawa, K. and Aoki, S. 2004, Photoperiod-regulated expression of the PpCOL1 gene encoding a homolog of CO/COL proteins in the moss *Physcomitrella patens*, *Biochem. Biophys. Res. Commun.*, **324**, 1296–301.
41. Hwang, I., Chen, H.C. and Sheen, J. 2002, Two-component signal transduction pathways in *Arabidopsis*, *Plant Physiol.*, **129**, 500–15.
42. Ishida, K., Niwa, Y., Yamashino, T. and Mizuno, T. 2009, A genome-wide compilation of the two-component systems in *Lotus japonicas*, *DNA Res.*, **16**, 237–47.